Dalton Transactions

Accepted Manuscript

ROYAL SOCIETY OF CHEMISTRY

www.rsc.org/dalton

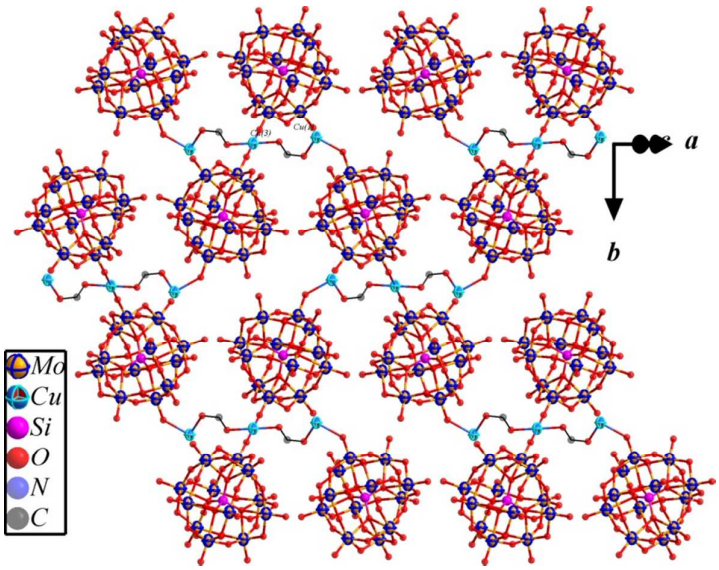

Six new compounds have been synthesized and characterized. Crystal structure analysis reveals that the six structures were tuned from 1-D to 2-D by using different secondary organic ligands.

Journal Name

RSCPublishing

ARTICLE

Cite this: DOI: 10.1039/x0xx00000x

Received 00th January 2012,
Accepted 00th January 2012

DOI: 10.1039/x0xx00000x

www.rsc.org/

Tuning the structures based on polyoxometalates from 1-D to 2-D by using different secondary organic ligands

Yang-Yang Hu[a], Xiao-Zhang*[b], De-Chuan Zhao[a], Hai-Yang Guo[a], Li-Wei Fu[a], Lan-Lan Guo[a], Xiao-Bing Cui*[a], Qi-Sheng Huo[a], Ji-Qing Xu[a]

Six new organic-inorganic hybrid compounds based on $[XM_{12}O_{40}]^{4-}$ (X=heteroatom, M= metal atom), namely $[Cu(pic)_2][H_2XM_{12}O_{40}]\cdot 2Hapy\cdot 2apy$ (X=Si, M=W for **1,** X =Ge, M =W for **2** and X=Si, M=Mo for **3**), $[Cu(2,2'\text{-bpy})_2][Cu(2,2'\text{-bpy})(H_2O)][Cu(pic)_2]_{0.5}[XM_{12}O_{40}]\cdot nH_2O$ (X=Si, M=Mo, n=0.5 for **4**, X=Ge, M=W, n=1 for **5**) and $[Cu(phen)(H_2O)]_2[Cu(pic)_2][GeW_{12}O_{40}]\cdot 2.5H_2O$ (**6**) (pic = deprotonated picolinic acid, apy = 2-aminopyridine, 2,2'-bpy=2,2'-bipyridine, phen= phenanthroline), have been synthesized and characterized by IR, UV-Vis, XRD, cyclic voltammetric measurements and single crystal X-ray diffraction analysis. Single crystal X-ray analysis reveals that compounds **1**-**3** are isomorphous and isostructural, in which each is based on $[H_2XM_{12}O_{40}]^{2-}$ and $[Cu(pic)_2]$. Compounds **4** and **5** are also isomorphous and isostructural, of which the structures are more interesting than those of compounds **1**-**3**. Both structures are constructed from $[XM_{12}O_{40}]^{4-}$ and metal mixed-organic-ligand complexes. Compound **6** is also constructed from Keggin ions and metal mixed-organic-ligand complexes, which is, however, thoroughly different from those of compounds **4** and **5**. The photodegradation properties of compounds **1**-**6** have been analyzed. Compounds **1**-**3** also exhibit rapid absorption properties for RhB (Rhodamine B). Detailed analysis of photodegradation properties of compounds **1**-**5** reveals that the molybdate POM has stronger degradation ability for RhB than the tungstate one.

Introduction

Polyoxometalates (POMs) form a distinctive class of inorganic metal-oxygen cluster compounds which is unique in its topological and electronic versatility and useful in fields as diverse as catalysis, analysis, biochemistry, materials science and medicine.[1] The class of POMs has been known for almost 200 years, but the first structural details were only revealed in the last century.[2] Up to now, the POM chemistry continues to be a considerable focus in the ongoing research because of the large number of novel POM structures and their properties. Many fundamental properties of the POM that have impact on its applications, including elemental composition, solubility, redox potential(s), charge density, size, and shape, etc., can be systematically altered to a considerable degree.[3]

Recent research interests are driven mainly by the introduction of abundant organic moieties or transition metal complexes (TMCs) into POMs.[4] Because they may adopt several roles: (a) as charge compensating subunits, (b) as covalently bonded subunits to the POM, (c) as inorganic bridges linking POMs into extended frameworks. The introduction of organic moieties or TMCs can not only enrich POM structures, but also ameliorate their polar, electricity, acid and redox properties. It is noted that most of above-mentioned POM-based compounds are constructed from POMs and N-containing moieties or metal N-containing ligand complexes.

We have focused on hybrids based on POMs and transition metal N-containing ligand complexes for years,[5] and we found that the TMC in the POM-based hybrid is almost always comprised of a type of metal ions and a type of organic ligands, but hybrids formed by POMs and transition metal mixed-organic-ligand complexes (TMMCs) are rather rare. From a design perspective, POM-based hybrids containing TMMCs could be divided into three types: namely type A, type B and type C. Type A hybrids contain more than one type of TMMC N-containing organic ligands;[6] type B hybrids contain more than one type of TMMC carboxylates; type C hybrids contain more than one type of TMMC organic ligands being composed of both N-containing organic ones and carboxylates.[7,8] To our knowledge, several type A hybrids were synthesized;[6] still no type B hybrids have been reported; type C compounds have been only rarely observed, [7,8] and carboxylates in these type C compounds are the simplest aliphatic dicarboxylate, namely oxalic acid[7] and the pyridinecarboxylate, namely isonicotinic acid.[8] It should be noted that the introduction of carboxylates into POMs has remained largely unexplored.[9] It might be attributed to the fact that there exists competition between POMs and carboxylates coordinating to metals. Obviously, it is still a challenging work to obtain hybrid compounds constructed from POMs and TMMCs containing carboxylates.

We attempt to synthesize all the above-mentioned three types of POM-based hybrids containing TMMCs. We have already synthesized some type A and type C hybrids.[5d, 10] We have pointed out that the synthesis of compounds constructed from

Table 1. crystal data and structural refinements for compounds **1** - **6**.

Empirical formula	$C_{32}H_{36}CuN_{10}O_{44}SiW_{12}$	$C_{32}H_{36}CuN_{10}O_{44}GeW_{12}$	$C_{32}H_{36}CuN_{10}O_{44}SiMo_{12}$	$C_{36}H_{31}Cu_{2.5}Mo_{12}N_7O_{43.5}Si$	$C_{36}H_{32}Cu_{2.5}GeN_7O_{44}W_{12}$	$C_{36}H_{35}Cu_3GeN_6O_{49.5}W_{12}$
Formula weight	3562.54	3606.95	2507.62	2595.90	3704.32	3813.04
Crystal system	triclinic	triclinic	triclinic	monoclinic	monoclinic	triclinic,
space group	P-1	P-1	P-1	P2(1)/n	P 2(1)/n	P -1
a (Å)	11.098(2)	11.110(2)	11.194(1)	13.8585(7)	13.880(2)	14.010(3)
b (Å)	12.728(3)	12.786(3)	12.702(1)	21.452(1)	21.660(3)	14.252(3)
c (Å)	13.176(3)	13.191(3)	13.162(2)	21.885(1)	21.898(3)	17.350(3)
α (°)	110.47(3)	110.394(3)	110.302(2)	90.00	90	99.63(3)
β (°)	97.61(3)	97.412(3)	98.157(2)	100.301(1)	100.354(2)	94.38(3)
γ (°)	111.72(3)	111.891(2)	111.880(2)	90.00	90	94.97(3)
Volume ($Å^3$)	1544.8(7)	1555.8(6)	1547.6(3)	6401.5(6)	6476.6(17)	3388.0(12)
Z	1	1	1	4	4	2
D_C ($Mg·m^{-3}$)	3.829	3.850	2.691	2.694	3.799	3.738
μ (mm^{-1})	22.702	22.996	2.811	3.202	22.576	21.740
F(000)	1581	1598	1197	4938	6566	3391
θ for data collection	3.07 to 29.05	3.06 to 29.09	1.74 to 25.00	1.34 to 28.43	2.96 to 29.15	2.91 to 29.11
Reflections collected	12854	13888	7773	40823	40698	32952
Reflections unique	7017	7152	5412	15828	14978	15650
R(int)	0.0321	0.0432	0.0245	0.0425	0.0608	0.0423
Completeness to θ	99.9	99.8	99.3	99.9	99.8	99.9
parameters	472	436	473	925	922	973
GOF on F^2	1.062	1.071	1.051	1.002	1.036	1.075
R^a [I>2σ(I)]	R_1 = 0.0695	R_1 = 0.0557	R_1 = 0.0876	R_1 = 0.0515	0.0514	0.0612
R^b (all data)	ωR_2 = 0.1468	ωR_2 = 0.1238	ωR_2 = 0.2250	ωR_2 = 0.1685	0.1211	0.1522

[a] $R_1 = \sum||F_0|-|F_c||/\sum|F_0|$. [b] $\omega R_2 = \{\sum [w (F_0^2-F_c^2)^2]/\sum[w(F_0^2)^2]\}^{1/2}$.

POMs and TMMCs of a N-containing ligand and a pyridinecarboxylate should be the breakthrough point for the synthesis of the above-mentioned second and third types of compounds.[10] After the syntheses of the compounds containing pyridinecarboxylates,[10] we want to further our study by introducing some new organic ligands. Therefore, we choose picolinic acid as the pyridinecarboxylate ligand and apy, 2,2'-bpy, and phen as N-containing organic ligands (secondary organic ligands) to explore the roles of these selected organic ligands in the synthesis of the hybrids.

Fortunately, we successfully prepared six novel complexes: $[Cu(pic)_2][H_2XM_{12}O_{40}]·2Hapy·2apy$ (X=Si, M=W for **1,** X =Ge, M =W for **2** and X=Si, M=Mo for **3**), $[Cu(2,2'\text{-bpy})_2][Cu(2,2'\text{-bpy})(H_2O)][Cu(pic)_2]_{0.5}[XM_{12}O_{40}]·nH_2O$ (X=Si, M=Mo, n=0.5 for **4**, X=Ge, M=W, n=1 for **5**), $[Cu(phen)(H_2O)]_2[Cu(pic)_2][GeW_{12}O_{40}]·2.5H_2O$ (**6**). Single crystal X-ray analysis reveals that compounds **1**-**3** are are isomorphous and isostructural, in which each is based on $[H_2XM_{12}O_{40}]^{2-}$ and $[Cu(pic)_2]$. It should be noted that compounds **1**-**3** did not contain TMMCs in them. Compounds **4** and **5** are also isomorphous and isostructural, of which the structures are more interesting than those of compounds **1**-**3**. The both structures are constructed from $[XM_{12}O_{40}]^{4-}$ and metal mixed-organic-ligand complexes. Compound **6** is also constructed from Keggin ions and metal mixed-organic-ligand complexes, which is, however, thoroughly different from those of compounds **4** and **5**. We found that the secondary organic ligand (apy, 2,2'-bpy or phen) is very important to the formation of the metal mixed-organic-ligand complex, and then the selection of the different secondary organic ligand will finally influence the final packing structure of the target compounds. The photodegradation properties of compounds **1**-**6** have been analyzed. Compounds **1**-**3** and compounds **4**-**5** are good examples to compare the photodegradation abilities of different POMs and the comparison reveals that the molybdate POM has stronger degradation ability for RhB than the tungstate one.

Experimental

All the chemicals used were of reagent grade without further purification. Infrared spectra were recorded as KBr pellets on a Perkin-Elmer SPECTRUM ONE FTIR spectrophotometer. UV-vis spectra were recorded on a Shimadzu UV3100 spectrophotometer. Powder XRD patterns were obtained with a Scintag X1 powder diffractometer system using Cu Kα radiation with a variable divergent slit and a solid-state detector. The electrochemical measurements were carried out on a CHI 660B electrochemical workstation.

$[Cu(pic)_2][H_2SiW_{12}O_{40}]·2Hapy·2apy$ (1) Compound **1** was synthesized hydrothermally by reacting of $H_4[\alpha\text{-}SiW_{12}O_{40}]·20H_2O$ (0.960g, 0.34mmol), $CuCl_2·2H_2O$ (0.340g, 2.0mmol), picolinic acid (0.062g, 0.51mmol), apy (0.056g, 0.59mmol) and distilled water (15ml) in a 18ml Teflon-lined autoclave. The resulting suspension was stirred for 3h and the pH of the mixture was necessarily adjusted to 5 with $NH_3·H_2O$ solution. The mixture was heated under autogenous pressure at 160°C for 5 days and then left to cool to room temperature. Dark green crystals could be isolated in about 40% yield (based on W). Anal. Calcd for $C_{32}H_{36}Cu_1N_{10}O_{44}Si_1W_{12}$: W, 61.93; Cu, 1.78; Si, 0.79; C, 10.79; H, 1.02; N, 3.93%. Found: W, 62.43; Cu, 1.60; Si, 0.68; C, 10.86; H, 1.03; N, 3.74%.

$[Cu(pic)_2][H_2GeW_{12}O_{40}]·2Hapy·2apy$ (2) Compound **2** was synthesized hydrothermally by reacting of $Na_2WO_4·2H_2O$ (0.660g, 2.0mmol), GeO_2 (0.105g, 1.0mmol), $CuCl_2·2H_2O$

(0.340g, 2.0mmol), picolinic acid (0.063g, 0.52mmol), apy (0.059g, 0.63mmol), acetic acid (1.0mL) and distilled water (15ml) in a 18ml Teflon-lined autoclave. The resulting suspension was stirred for 3h and the pH of the mixture was 4. The mixture was heated under autogenous pressure at 160°C for 5 days and then left to cool to room temperature. Dark green crystals could be isolated in about 65% yield (based on W). Anal. Calcd for $C_{32}H_{36}Cu_1Ge_1N_{10}O_{44}W_{12}$: W, 61.16; Cu, 1.76; C, 10.66; H, 1.01; N, 3.88%. Found: W, 60.43; Cu, 1.70; C, 10.86; H, 0.83; N, 3.94%.

$[Cu(pic)_2][H_2SiMo_{12}O_{40}]\cdot 2Hapy\cdot 2apy$ (3) Compound **3** was synthesized hydrothermally by reacting of $Na_2MoO_4\cdot 2H_2O$ (0.484g, 2.0mmol), $Na_2SiO_3\cdot 9H_2O$ (0.284g, 1.0mmol), $CuCl_2\cdot 2H_2O$ (0.340g, 2.0mmol), picolinic acid (0.062g, 0.51mmol), apy (0.073g, 0.78mmol), HCl (1.0mL) and distilled water (15ml) in a 18ml Teflon-lined autoclave. The resulting suspension was stirred for 3h and the pH of the mixture was necessarily adjusted to 2 with HCl solution. The mixture was heated under autogenous pressure at 160°C for 5 days and then left to cool to room temperature. Dark green crystals could be isolated in about 58% yield (based on Mo). Anal. Calcd for $C_{32}H_{36}Cu_1N_{10}O_{44}Si_1Mo_{12}$: Mo, 45.91; Cu, 2.53; Si,1.12; C, 15.33; H, 1.45; N, 5.59%. Found: Mo, 45.43; Cu, 2.40; Si, 1.18; C, 14.86; H, 1.23; N, 5.54%.

$[Cu(2,2'\text{-}bpy)_2][Cu(2,2'\text{-}bpy)(H_2O)][Cu(pic)_2]_{0.5}[SiMo_{12}O_{40}]\cdot 0.5H_2O$ (4) Compound **4** was synthesized hydrothermally by reacting of $Na_2MoO_4\cdot 2H_2O$ (0.484g, 2.0mmol), $Na_2SiO_3\cdot 9H_2O$ (0.284g, 1.0mmol), $CuCl_2\cdot 2H_2O$ (0.341g, 2.0mmol), picolinic acid (0.063g, 0.52mmol), 2,2'-bpy (0.078g, 0.50mmol), HCl (1.0mL) and distilled water (15ml) in a 18ml Teflon-lined autoclave. The resulting suspension was stirred for 3h and the pH of the mixture was 3.5. The mixture was heated under autogenous pressure at 160°C for 5 days and then left to cool to room temperature. Green crystals could be isolated in about 43% yield (based on Mo). Anal. Calcd for $C_{36}H_{31}Cu_{2.5}N_7O_{43.5}Si_1Mo_{12}$: Mo, 44.35; Cu, 6.12; Si,1.08; C, 16.66; H, 1.20; N, 3.78%. Found: Mo, 44.43; Cu, 6.20; Si, 0.97; C, 16.39; H, 1.00; N, 3.69%.

$[Cu(2,2'\text{-}bpy)_2][Cu(2,2'\text{-}bpy)(H_2O)][Cu(pic)_2]_{0.5}[GeW_{12}O_{40}]\cdot H_2O$ (5) Compound **5** was synthesized hydrothermally by reacting of $Na_2WO_4\cdot 2H_2O$ (0.660g, 2.0mmol), GeO_2 (0.110g, 1.0mmol), $CuCl_2\cdot 2H_2O$ (0.343g, 2.0mmol), picolinic acid (0.124g, 1.0mmol), 2,2'-bpy (0.078g, 0.50mmol), NaOH (0.081g, 2.0mmol) and distilled water (15ml) in a 18ml Teflon-lined autoclave. The resulting suspension was stirred for 3h and the pH of the mixture was necessarily adjusted to 1.5 with HCl solution. The mixture was heated under autogenous pressure at 160°C for 3 days and then left to cool to room temperature. Green block crystals could be isolated in about 48% yield (based on W). Anal. Calcd for $C_{36}H_{32}Cu_{2.5}N_7O_{44}Ge_1W_{12}$: W, 59.56; Cu, 4.29; C, 11.67; H, 0.87; N, 2.65%. Found: W, 59.11; Cu, 4.19; C, 11.55; H, 0.93; N, 2.81%.

$[Cu(phen)(H_2O)]_2[Cu(pic)_2][GeW_{12}O_{40}]\cdot 2.5H_2O$ (6) Compound **6** was synthesized hydrothermally by reacting of $Na_2WO_4\cdot 2H_2O$ (0.661g, 2.0mmol), GeO_2 (0.210g, 2.0mmol), $CuCl_2\cdot 2H_2O$ (0.342g, 2.0mmol), picolinic acid (0.123g, 1.0mmol), phen (0.10g, 0.50mmol) and distilled water (15ml) in a 18ml Teflon-lined autoclave. The resulting suspension was stirred for 3h and the pH of the mixture was necessarily adjusted to 1.5 with HCl solution. The mixture was heated under autogenous pressure at 160°C for 3 days and then left to cool to room temperature. Blue block crystals could be isolated in about 35% yield (based on W). Anal. Calcd for $C_{36}H_{33}Cu_3GeN_6O_{48.5}W_{12}$: W, 57.86; Cu, 5.00; C, 11.34; H, 0.93; N, 2.20%. Found: W, 58.42; Cu, 4.89; C, 11.34; H, 0.83; N, 2.14%.

Preparations of 1-, 2-, 3-, 4-, 5-, and 6-CPEs. The compound 1-modified carbon-paste electrode (1-CPE) was fabricated as follows: 6 mg graphite powder, 1 μL of Nujol and 3 mg compound **1** were blended and grounded thoroughly in an agate mortar. Then the homogeneous mixture was packed into a poly(tetrafluoroethylene) tube with a 1.5 mm inner diameter, and the tube surface was wiped with paper. Electrical contact was established with a Cu rod through the back of the electrode. In a similar manner, **2**-, **3**-, **4**-, **5**-, and **6**-CPEs were made with compounds **2**-**6**. Electrochemical measurements were performed with a CHI 660b electrochemical workstation. A conventional three-electrode system was used with Ag/AgCl as a reference electrode and Pt wire as a counter electrode. Chemically bulk-modified CPEs were used as the working electrodes. CV measurements are carried out in a 1 mol/L H_2SO_4 aqueous solution.

The reflection intensity data for compounds **1**, **2**, **5** and **6** were collected on an Agilent Technology Super Nova Eos Dual system with a (Mo-K_α, λ = 0.71073Å) microfocus source and focusing multilayer mirror optics. Data were collected under ambient conditions. Data collections, unit cell determinations and refinements, absorption corrections and data reductions were performed using the CrysAlisPro software from Agilent Technologies. The analytical absorption correction was performed by applying a face-based absorption correction as well as a spherical absorption correction. Compounds **3** and **4** were measured on a Bruker Apex II diffractometer with a graphite monochromated Mo K_α (λ = 0.71073Å) radiation source. None of the crystals showed evidence of crystal decay during data collections. Refinement was carried out with SHELXS-2014/7[11] and SHELXL-2014/7[11] using WinGX via the full matrix least-squares on F_2 method.[12] In the final refinements, all atoms were refined anisotropically in compounds **1**-**6**. A summary of the crystallographic data and structure refinements for compounds **1**-**6** is given in Table **1**. CCDC number: 1056231 for **1,** 1056232 for **2,** 1056233 for **3,** 1056234 for **4**, 1403342 for **5** and 1403343 for **6**. These data can be obtained free of charge from The Cambridge Crystallographic Data Centre *via* www.ccdc.cam.ac.uk/data_request/cif.

Results and discussion

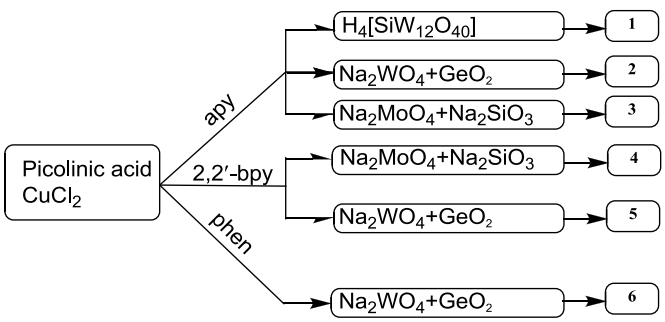

Scheme 1. Summary of the reactions of compounds **1**-**6**.

As shown in scheme 1, all the six compounds are synthesized by using the picolinic acid and a rigid N-heterocyclic ligand. Compounds **1**-**3** were synthesized under similar conditions; especially the molar ratios of picolinic acid/$CuCl_2\cdot 2H_2O$/apy for the three compounds are almost identical. Moreover, compound

1 was synthesized by adding $\{SiW_{12}O_{40}\}$ as one starting material directly, of which the structural integrity was maintained throughout the construction process. Compounds **2** and **3** were synthesized by the additions of corresponding metal oxides to prepare in situ POMs in the two products. The molar ratios of the corresponding metal oxides for compounds **2** and **3** are identical too.

The molar ratios of picolinic acid/$CuCl_2{\cdot}2H_2O$/secondary organic ligand/corresponding metal oxides for compounds **2-4** are almost identical except that apy was replaced by 2,2'-bpy in the preparation of compound **4**. The molar ratios of picolinic acid/$CuCl_2{\cdot}2H_2O$/secondary organic ligand/corresponding metal oxides for compounds **5-6** are almost identical but with some differences from those of compounds **2-4**: the number of moles of picolinic acid used for compounds **5-6** is twice as many as that used for compounds **2-4.** More importantly, the secondary organic ligand in compounds **4-6** is thoroughly different from that in compounds **1-3**.

In the preparations of compounds **1-3**, apy is added as the secondary organic ligand, and fortunately, it has been successfully introduced into POMs. However, the introduced apy did not coordinate to copper ions in compounds **1-3**, but only act as the dissociated organic moiety filling spaces.

Actually, the syntheses of both compounds **1-3** and compounds **4-6** demonstrated that the introduction of carboxylates into POMs is successful. However, compounds **1-3** are based on POMs and metal complexes containing only one kind of carboxylates and compounds **4-6** are based on POMs and TMMCs of one carboxylate and one N-containing ligand. That is to say, to synthesize the type C compounds above-mentioned, not only the carboxylate selected is important, but also the secondary N-containing ligand is important too.

For compound **4 (5** or **6)**, 2,2'-bpy (or phen) form a chelate ring with a copper ion, the copper of the chelate complex was then coordinated by one carboxylate oxygen from pic^-, and the other carboxylate oxygen of pic^- coordinates to another copper ion. Therefore, pic^- here as a μ_2-bridge links two copper ions into a novel TMMC. However, pic^- in compounds **1-3** also coordinates to a copper ion into a chelate complex, however, there did not exist the secondary chelating ligand like 2,2'-bpy in compound **4 (5)** or phen in compound **6**, so the Cu-pic chelate complex in compounds **1-3** cannot be further linked to other copper ions to form TMMC just like that in compound **4 (5** or **6)**.

The secondary organic ligand should be the main reason of the difference among the six structures. Compounds **1-6** were synthesized under similar acidic conditions, in each of which there should be similar proportions of protonated picolinate ligands. All the six compounds are based on $[XM_{12}O_{40}]^{4-}$, thus the counterions in compounds **1-3** should be only one kind of copper complexes for apy or Hapy cannot form a chelate complex with the copper ion, and protons have to be used as counterions to balance the charge. However, for compounds **4-6**, not only the picolinate can form chelate complex with the copper ion, but also the secondary N-containing organic ligand can form chelate complex with the copper ion, therefore, in the reaction mixtures for compounds **4-6**, there should be two different complexes as counterions, which are the copper picolinate complex and copper 2,2'-bpy (phen) complex, therefore, there are enough cations in the reaction mixtures, and the assembly of the polynuclear TMMC is possible.

We also tried to use 4,4'-bpy as the secondary organic ligand to prepare similar compounds to compounds **4-6**, but unfortunately, suitable crystals for X-ray analysis were not obtained yet.

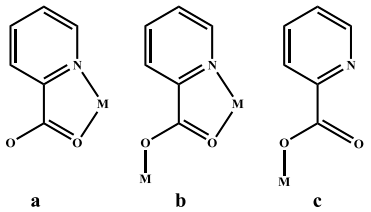

Scheme 2. Coordination modes of used picolinic acid in the six compounds.

Pic^- exhibits three coordination modes as shown in scheme 2.[16] all the pic^- ligands in compounds **1-3** adopt the first one, whereas all the pic^- ligands in compounds **4-6** exhibit the second one. It should be noted that pic^- in the compound that is similar to compounds **4-6** reported by us very recently, also adopts the second coordination mode.[10]

Crystal structure of 1. The crystal structures of compounds **1-3** are isomorphous and isostructural, belonging to the triclinic space group P-1. Here compound **1** was detailedly described as an example.

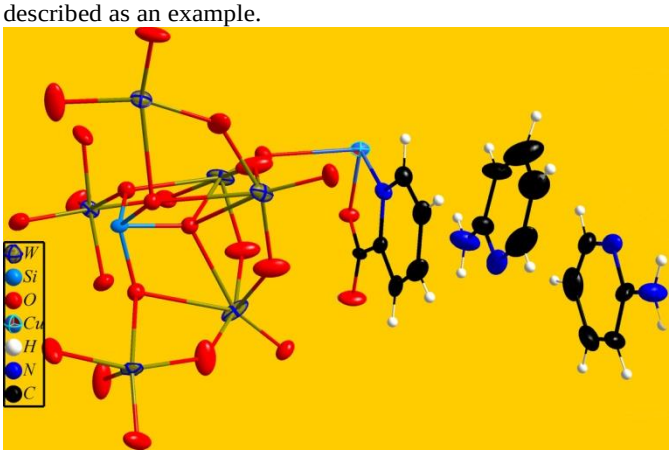

Fig. 1 ORTEP view of the asymmetric unit of compound **1** with 30% ellipsoid probability.

The Keggin core in compound **1** includes a $\{SiO_4\}$ surrounded by twelve $\{WO_6\}$ arranged in four groups of three edge-sharing octahedra units $\{W_3O_{13}\}$. W-O bonds can be classified into three sets: W-O_t (terminal oxygens) with distances of 1.65(2)-1.69(2)Å, W-O_b (bridging oxygens) with distances of 1.86(2)-1.94(2)Å and W-O_c (central oxygens) with distances of 2.31(4)-2.36(3)Å. Oxidation states for W atoms were calculated using the parameters given by Brown.[13] Results indicate that all the tungsten atoms are in the +6 oxidation state.

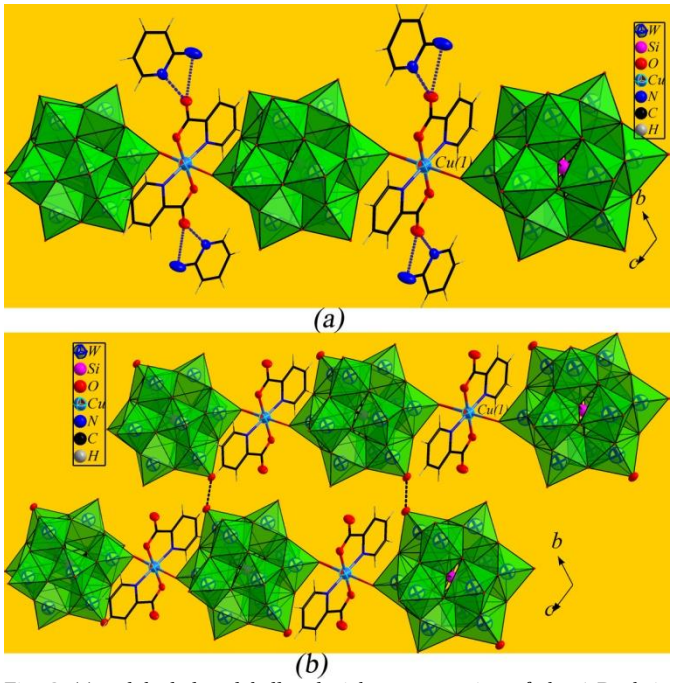

Fig. 2 (a) polyhedral and ball-and-stick representation of the 1-D chain structure formed by POMs and $[Cu(pic)_2]$ ions; (b) polyhedral and ball-and-stick representation of the 2-D structure in compound **1**.

The asymmetric unit of compound **1** is composed of half a $[H_2SiW_{12}O_{40}]^{2-}$, half a $[Cu(pic)_2]$, a Hapy and an apy moieties. As shown in Fig. 1, $[Cu(pic)_2]$ consists of a copper ion which is chelated by two pic^- via the heterocyclic nitrogen and one of the carboxylate oxygens. The Cu-N and Cu-O distances are 1.94(2)Å and 1.95(2)Å, respectively. Though pic^- has three donor atoms, it only serves as a bidentate ligand. On the other hand, Cu(1) adopts an octahedral geometry with two nitrogens and two oxygens from two pic^- forming the equatorial plane and two oxygens from two $[H_2SiW_{12}O_{40}]^{2-}$ occupying the two apical positions with a Cu-O distance of 2.5459(8)Å. Therefore, $[Cu(pic)_2]$ acting as a bridge connects $[H_2SiW_{12}O_{40}]^{2-}$ into a novel 1-D chain structure running along the (0, 1, 1) direction. The structure of compound **1** is reminiscent of the structures constructed from POMs and $[M(NL)_2]^{n+}$ (NL = N-containing chelating ligand, e.g., ethylenediamine and phen. The role of NL is identical to that of pic^- that serves as a chelating ligand binding the metal center to form a five-membered chelate ring)[5a, 14] which have been thoroughly explored over the past years. However, similar POM-based hybrids with $[M(CL)_2]^{n+}$ (CL = bidentate chelating carboxylate ligand or N-heterocyclic carboxylate ligand that plays the same role as pic^-) as the linking agent are rarely observed. To our knowledge, one such compound based on $\{Mo_8O_{26}\}$ and $[M(pzca)_2]^{n+}$ (pzca = 2-pyrazinecarboxylic acid) has been reported very recently.[15] There were also three compounds containing $[M(nic)_2]^{n+}$ (nic^- = nicotinic acid) or $[M(inic)_2]^{n+}$ ($inic^-$ = isonicotinic acid) reported previously,[16] however, detailed analysis found that neither nic^- nor $inic^-$ serves as a bidentate chelating ligand, but a monodentate one coordinating to the metal center.[16] Furthermore, POM-based compounds containing bipyridine based bis(TRIS) ligands which are analogous to pic^- have also been reported,[15] however, these analogous ligands did not bind a metal ion to form a $[M(CL)_2]^{n+}$ complex.[17]

The other of the carboxylate oxygens of pic^- participates in two N-H···O hydrogen bonding interactions with two nitrogens from a Hapy with N···O distances of 2.707(1)-2.8402(8)Å. Alternatively, the two nitrogens from the Hapy form a five-membered ring with the carboxylate oxygen, which can increase the stability of these two hydrogen bonds, as shown in Fig. 2(a). Except for the hydrogen bonds involving Hapy and pic^-, there is another N-H···O hydrogen bond, of which the amino nitrogen of apy acts as hydrogen donor and a $[H_2SiW_{12}O_{40}]^{2-}$ oxygen acts as the hydrogen acceptor with N···O distance of 2.8005(9)Å. There are no strong C-H···O hydrogen-bonding interactions either between carbons of $[Cu(pic)_2]$ and oxygens of $[H_2SiW_{12}O_{40}]^{2-}$ or between carbons of Hapy or apy and oxygens of $[H_2SiW_{12}O_{40}]^{2-}$. Detailed analysis only found a weak C-H···O hydrogen bond between C(2) from $[Cu(pic)_2]$ and O(15) from $[H_2SiW_{12}O_{40}]^{2-}$ with a C···O distance of 2.994(1)Å and a C-H···O angle of 98.12(3)º.

Except for N-H···O hydrogen bonding interactions, there also exist O-H···O hydrogen bonds, which can direct the assembly of the 1-D chains into a 2-D layer. As shown in Fig. 2(b), O(10) from a POM interacts with O(10a, a:-x, 1-y, 1-z) from another POM with a O···O distance of 2.9561(7)Å, which is in the range of O-H···O hydrogen bonds. It should be noted that the Keggin POM in compound **1** is diprotonated; the positions of the two hydrogen atoms are hard to be determined using the crystal analysis. However, from the strong hydrogen bonds between O(10) and O(10a), it is very clear that the O(10) and its symmetry equivalent are the obvious sites where the two protons can be attached.

The structure of compound **2** is almost identical to that of compound **1**; even hydrogen bond distances and angles are almost identical to those of compound **1**. The reason is that Ge and Si belong to the same main group and the two are enclosed in the same metal shell.

The structure of compound **3** has some slight differences from those of compounds **1** and **2**. The apy moiety in compound **3** is not similar to those in compounds **1** and **2**, two nitrogens from apy form a five-membered ring with one carboxylate oxygen in compounds **1** and **2**, however, the apy in compound **3** is not similar to those in compounds **1** and **2,** only one nitrogen of which participates in the hydrogen bond with a carboxylate oxygen with a N···O distance of 2.8401(2)Å.

Crystal structures of 4 and 5. Compounds **4** and **5** are isomorphous and isostructural, hence compound **4** was described in detail below. The asymmetric unit of compound **4** is comprised of a $[SiMo_{12}O_{40}]^{4-}$, half a copper-aqua-2,2-bipyridine-picolinate complex $[Cu_3(2,2'\text{-bpy})_2(pic)_2(H_2O)_2]^{4+}$, a copper-2,2-bipyridine complex $[Cu(2,2'\text{-bpy})_2]^{2+}$ and a lattice water molecule.

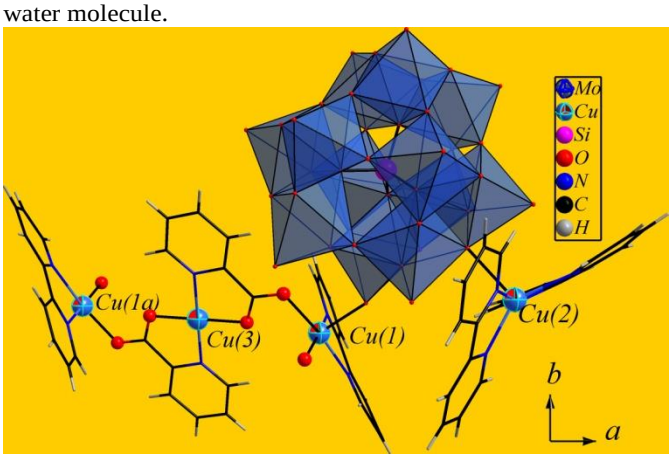

Fig. 3 polyhedral and ball-and-stick representation of the copper-aqua-2,2-bipyridine-picolinate complex, copper-2,2-bipyridine complex and the POM in compound **4**. Symmetry code: a (-1-x,-y,1-z).

The copper-aqua-2,2-bipyridine-picolinate complex comprises three copper ions, two 2,2'-bpy, two pic$^-$ and two coordinated water molecules. As shown in Fig. 3, Cu(3) occupies the inversion center of the TMMC. pic$^-$ not only coordinates to Cu(3) in a bidentate chelating manner via the heterocyclic nitrogen and one of the carboxylate oxygens, but also simultaneously coordinates to Cu(1) in a monodentate coordination mode via the other of the carboxylate oxygens. The Cu-N distance is 1.975(6)Å and Cu-O distances are 1.952(6)-1.984(5)Å. Thus, pic$^-$ acting as a tridentate μ_2-ligand through all the three donor atoms links the two crystallographically independent copper centers of the TMMC. The coordination mode of pic$^-$ in compound **4** is different from that of pic$^-$ in compound **1**. The two pic$^-$ oxygens are each bonded to one copper ion in compound **4**, whereas only one of the two corresponding oxygens of pic$^-$ in compound **1** is bound to one copper ion. Therefore, pic$^-$ serves as a tridentate μ_2-bridge in compound **4**, whereas pic$^-$ in compound **1** only serves as a terminal ligand. N(1) 2,2'-bpy coordinates to Cu(1) via its two nitrogens in a chelating fashion with Cu-N distances of 1.973(7)-1.987(8)Å. On the other hand, Cu(3) exhibits an octahedral geometry, with two nitrogens and two carboxylate oxygens from two pic$^-$ forming the basal plane and two oxygens from two $[SiMo_{12}O_{40}]^{4-}$ being located at the two apical positions with a Cu-O distance of 2.380(5)Å, indicating that $[Cu(3)(pic)_2]$ acting as a bridge joining $[SiMo_{12}O_{40}]^{4-}$. The role of Cu(3) here is very similar to that of copper in compounds **1**, which serves as a bridge linking POMs. Cu(1) adopts a square-pyramidal geometry for the N_2O_3 donor set, where the basal coordination sites are occupied by two 2,2'-bpy nitrogens, one carboxylate oxygen from pic$^-$ and one lattice water molecule Ow(1) and the apical site is occupied by an oxygen from $[SiMo_{12}O_{40}]^{4-}$ with a Cu-O distance of 2.278(5)Å. Ow(1) as a terminal ligand coordinates to Cu(1) with a Cu-O distance of 1.957(6)Å. In one word, pic$^-$ plays the most important role for the formation of TMMC, which links two $[Cu(2,2'\text{-bpy})]^{2+}$ and Cu(3) into a novel TMMC.

Thus, the main difference between compounds **1** and **4** is the introduction of different secondary organic moieties. In compound **1**, the secondary organic moiety is apy (Hapy), which is not a chelating ligand and cannot coordinate to a copper ion to form a metal complex. $[Cu(pic)_2]$ in compound **1** then joins POMs only into a 1-D chain structure. The introduction of 2,2'-bpy in compound **4** make a main difference: 2,2'-bpy coordinates to a copper ion into a $[Cu(2,2'\text{-bpy})]^{2+}$ and then two $[Cu(2,2'\text{-bpy})]^{2+}$ are linked by $[Cu(pic)_2]$ into a trinuclear TMMC. And more importantly, all the three copper ions interact with surrounding $[SiMo_{12}O_{40}]^{4-}$ via strong covalent bonds, therefore, trinuclear TMMCs and POMs are linked into a novel 2-D layer framework structure.

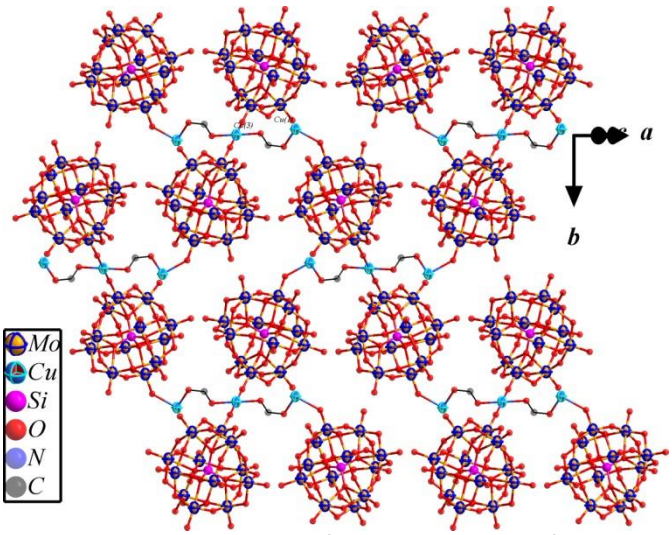

Fig. 4 ball-and-stick representation of the 2-D layer structure of compound **4**. Carbons except C(35), nitrogens, supported Cu(2) ions and water molecules are omitted for clarity.

The role of Cu(3) is most important in the formation of the TMMC, which is coordinated by two pic$^-$ and then the two pic$^-$ respectively acting as a μ_2-bridge joining Cu(3), Cu(1) and Cu(3), Cu(1a). Therefore, a trinuclear TMMC was formed. As shown in Fig. 4, each TMMC interacts with four POMs via Cu-O contacts, while each POM only interacts with two TMMCs, thus a novel 2-D layer structure constructed from POMs and TMMCs was formed. The repeating unit of the 2-D layer is constructed from four POMs and four TMMCs.

Cu(2) displays a trigonal bipyramidal geometry rather than the octahedral geometry around Cu(3) and the pyramidal geometry around Cu(1). Cu(2) is coordinated by four nitrogens from two 2,2'-bpy ligands with Cu-N distances of 1.950(6)-2.029(6)Å and one terminal oxygen from $[SiMo_{12}O_{40}]^{4-}$ with a Cu-O distance of 2.410(5)Å. Alternatively, POM acting as terminal ligand coordinates to Cu(2), forming a POM supported copper complex. Therefore, Cu(2) complex acts as a terminal unit grafted on the surface of $[SiMo_{12}O_{40}]^{4-}$.

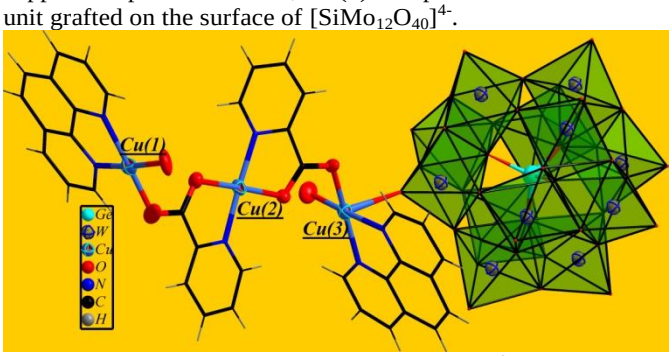

Fig. 5 polyhedral and ball-and-stick representation of the copper-aqua-phenanthroline-picolinate complex and the POM in compound **6**.

Crystal structure of compound 6. X-ray analysis shows that the asymmetric unit of compound **6** is comprised of a $[GeW_{12}O_{40}]^{4-}$, a copper-aqua-phenanthroline-picolinate complex $[Cu_3(phen)_2(pic)_2(H_2O)_2]^{4+}$ and two lattice water molecules.

The formula of the TMMC in compound **6** is very similar to that of the TMMC in compound **4**; the main difference between the two is phen replacing 2, 2'-bpy. The structures of the two TMMCs are also very similar to each other. As shown in Fig. 5, TMMC in compound **6** comprises three copper ions, two phen, two pic$^-$ and two coordinated water molecules. pic$^-$ in compound **6** plays the same role as that in compound **4**, acting

as a tridentate μ_2-ligand joining two copper ions. phen in compound **6** also plays the same role as 2,2'-bpy in compound **4**, acting as a terminal ligand with a copper ion forming a chelate complex. Therefore, the structure of the TMMC in compound **6** is very similar to the TMMC in compound **4**.

The roles of the three copper centers in compound **6** are not fully identical to those in compound **4**. The two copper ions chelated by two phen in compound **6** exhibit a square-pyramidal geometry which is identical to those around the two corresponding copper ions in compound **4**, however, the copper ion chelated by pic$^-$ in compound **6** presents a square-pyramidal geometry rather than the corresponding octahedral geometry in compound **4**. Therefore, copper ions in the TMMC in compound **6** only interact with three surrounding Keggin POMs, but not four surrounding Keggin POMs like those in compound **4**.

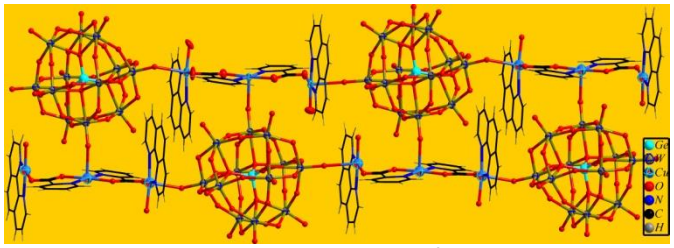

Fig. 6 ball-and-stick and wire representation of the 1-D double-chain in compound **6**.

The role of the Keggin POM in compound **6** is also different from those in compound **4**. Each POM in compound **6** interacts with three TMMCs, but each POM in compound **4** only interacts with two TMMCs. Thus, the extended structure of compound **6** constructed from POMs and TMMCs is thoroughly different from that in compound **4**, which exhibits a novel double-chain structure as shown in Fig. 6. Cu(1) and Cu(3) of TMMC each interact with two $[GeW_{12}O_{40}]^{4-}$ with Cu-O distances of 2.34(1)-2.37(1)Å via Cu(1)-O and Cu(3)-O interactions, alternatively, $[GeW_{12}O_{40}]^{4-}$ was linked by TMMCs into a novel 1-D straight chain structure running along the (0, 1, -1) direction. Cu(2) of TMMC only interacts with one $[GeW_{12}O_{40}]^{4-}$ from another chain with a Cu-O distance of 2.45(1)Å, thus, two chains are connected into a novel double-chain structure via Cu(2)-O contacts.

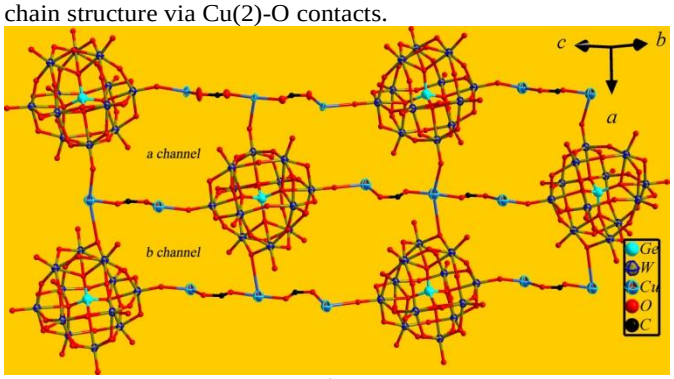

Fig. 7 ball-and-stick representation of the 2-D layer in compound **6**. Carbons except C(35) and C(36), nitrogens and coordinated water molecules are omitted for clarity.

Though the three crystallographically independent copper ions all adopt a square-pyramidal geometry, the geometry of Cu(2) seems to be different from the other two. The sixth coordination site of Cu(1) or Cu(3) cannot be occupied by an extra atom for the steric hindrance of pic$^-$. However, the sixth coordination site of Cu(2) can be occupied by an extra oxygen from another double-chain with a Cu-O distance of 3.0537(7)Å, indicating that the Cu-O interaction is very weak. Thus, the double-chains are linked via weak Cu(2)-O contacts into a novel 2-D layer structure. There are two types of channels in the 2-D layer. As shown in Fig. 7, the a type is constructed from two POMs and two halves of TMMCs via covalent Cu(2)-O interactions with dimensions of 8.47×8.82Å, whereas the b type is formed by two POMs and two halves of TMMCs via weak Cu(2)-O contacts with dimensions of 9.10×5.81Å.

There are only one type of channels in the layer of compound **4** which is made up of four POMs and four halves of TMMCs. Why the channels of compounds **4** and **6** are so different? We think the different secondary organic ligands should be the main reason, it is 2,2'-bpy in compound **4** and phen in compound **6**. The square-pyramidal geometry around the two copper ions coordinated by 2,2'-bpy in the TMMC of compound **4** are more distorted than that around the two corresponding copper ions coordinated by phen in compound **6**. More importantly, there is still an extra $[Cu(2,2'\text{-bpy})_2]^{2+}$ in compound **4**, which will influence the coordination modes of the POM and the TMMC in compound **4** greatly. However, it is still elusive why compound **6** did not contain a similar complex.

The structures of compounds **4**-**6** are reminiscent of the compound we reported very recently.[10] The formula of the reported compound is $[Cu_2(pic)(2,2'\text{-bpy})_2Cl]_2[SiW_{12}O_{40}]$, the main difference in the formulas between compound **4** and the reported compound is the TMMC water in compound **4** replacing the TMMC chloride in the reported compound. The structure of compound **4** are thoroughly different from that of the reported compound, the reported compound is only a discrete polyoxometalate supported copper-2,2'-bpy-chloro-nicotinate complex. The differences in the formulas of compound **6** and the reported compound are the TMMC phen and water in compound **6** replacing the TMMC 2,2'-bpy and chloride in the reported compound. In conclusion, the structures of compounds **4**, **6** and the reported compound are thoroughly different from one another.

Characterization

Compounds **1-6** contain similar Keggin POMs. Therefore, IR spectra of them are very similar. The IR spectrum of compound **1** was detailedly described as an example. The IR spectrum of compound **1** is shown in Fig. s1, of which the characteristic band at 973cm^{-1} is attributed to υ(W-O$_t$), the band at 882 cm^{-1} is ascribed to υ(W-O$_b$-W), and the band at 792cm^{-1} is due to υ(W-O$_c$), respectively. The stretching of Si-O bonds is observed at the spectrum band of 921cm^{-1}.[18] The absorption bands at 1667-1166cm^{-1} are due to vibrations of pic$^-$, Hapy and apy moieties in compound **1**. The IR spectra of compounds **2**, **5** and **6** are similar to that of compound **1**, which exhibit characteristic bands at 971, 884, 780cm^{-1} for **2**, 970, 883, 780cm^{-1} for **5** and 974, 885, 781cm^{-1} for **6** ascribed to υ(W-O$_t$), υ(W-O$_b$-W) and υ(W-O$_c$), respectively,[18] the stretching vibrations of Ge-O bonds are observed at the spectrum bands of 828cm^{-1} for **2**, 829 cm^{-1} for **5** and 829 cm^{-1} for **6**, respectively. Bands from 1668-1099cm^{-1} for **2**, 1589-1108cm^{-1} for **5** and 1587-1111cm^{-1} for **6** are assigned to pic$^-$, Hapy and apy moieties in compound **2** and pic$^-$ and phen moieties in compounds **5** and **6**, respectively. Compounds **3** and **4** contain the identical $[SiMo_{12}O_{40}]^{4-}$, therefore, the two spectra are similar, both of which exhibit similar bands at 946, 901, 859, 787cm^{-1} for compound **3** and 948, 901, 867, 792cm^{-1} for compound **4** corresponding to υ(Mo-O$_t$), υ(Si-O$_c$), υ(Mo-O$_b$-Mo) and υ(Mo-O$_c$). Bands from 1643-1099cm^{-1} for compound **3** and 1590-1108cm^{-1} for compound **4** are assigned to pic$^-$, Hapy and apy moieties in compound **3** and pic$^-$ and 2,2'-bpy ligands in compound **4**.

The X-ray powder diffraction patterns of compounds **1-6** are all in good agreement with the simulated XRD patterns, confirming the phase purity of all the four compounds (Fig. s2). The differences in reflection intensities are probably due to preferential orientations in the powder samples of compounds **1-6**.

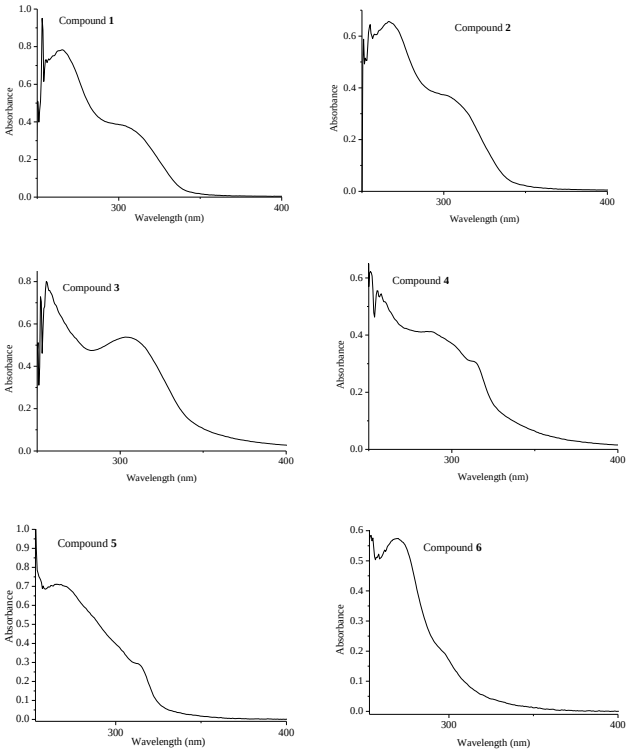

Fig. 8 UV-Vis spectra of compounds **1-6**.

UV-Vis spectra of compounds **1-6**, in the range of 250-400 nm, are presented in Fig. 8. The UV-Vis spectrum of compound **1** displays an intense broad absorption peak centered at about 265nm with one shoulder peak at about 303nm assigned to O→W charge transfer and n→π* transitions of the apy moiety and piclinic ligand in compound **1**. UV-Vis spectra of compounds **2, 5** and **6** exhibit very similar intense broad absorption peaks and shoulder peaks to that of compound **1** centered about 266, 303nm, 267, 312nm and 269, 297nm, which should be ascribed to charge transfer transitions of O→W and n→π* transitions of organic ligands in compounds **2, 5** and **6**, respectively. However, UV-Vis spectra of compounds **3** and **4** show some differences from that of compound **2.** The POM species in compound **3** is different from those of compounds **1 2**, **5** and **6**, therefore, the UV-Vis spectrum of compound **3** is different from those of compounds **1 2**, **5** and **6**. The UV-Vis spectrum of compound **3** shows an absorption peaks centered at about 255nm and a shoulder peak at about 303nm, which should be due to the charge transfer transition of O→Mo and n→π* transitions of organic ligands in compound **3**. The UV-Vis spectrum of compound **4** is different from the other five, which shows an absorption peak at about 255nm and two shoulder peaks at about 287 and 313nm, being consistent with the charge transfer transition of O→Mo and n→π* transitions of organic ligands in compound **4**. In conclusion, both POMs and organic moieties will importantly influence the final UV-Vis spectra. Compounds **1** and **2** contain almost identical POMs and identical organic moieties, thus, the spectra of the two are almost identical with only slight differences. Compounds **5** and **6** contain similar POMs to those of compounds **1** and **2**, therefore, the peaks ascribed to the O→W charge transfer transition are similar to those of compounds **1** and **2**. Compound **3** contains only identical organic moieties to those of compounds **1** and **2** but different POMs from those of compound **1** and **2**, thus, only spectra peaks due to n→π* transitions of organic ligands of the three are similar. Compound **4** contains diffrent organic moieties from those of compounds **1-3**, indicating that spectrumn peaks corresponding to n→π* transitions of organic ligands in compound **4** are different from those of compounds **1-3**. However, compounds **3** and **4** contain the same POM species, thus the spectra peaks ascribed to the O→Mo charge transfer transition are similar to each other. Compound **5** contains identical organic moieties to those of compound **4**, thus, the UV-Vis peaks of the two exhibit similar peaks at 312 and 313nm respectively. The hidden peak at about 287nm for compound **5** is overlapped with the O→W charge transfer peak. Compound **6** contains different organic moieties to those of compounds **1-5**. The UV-Vis peak due to n→π* transitions of organic ligands in compound **6** is thus different from those of the other five.

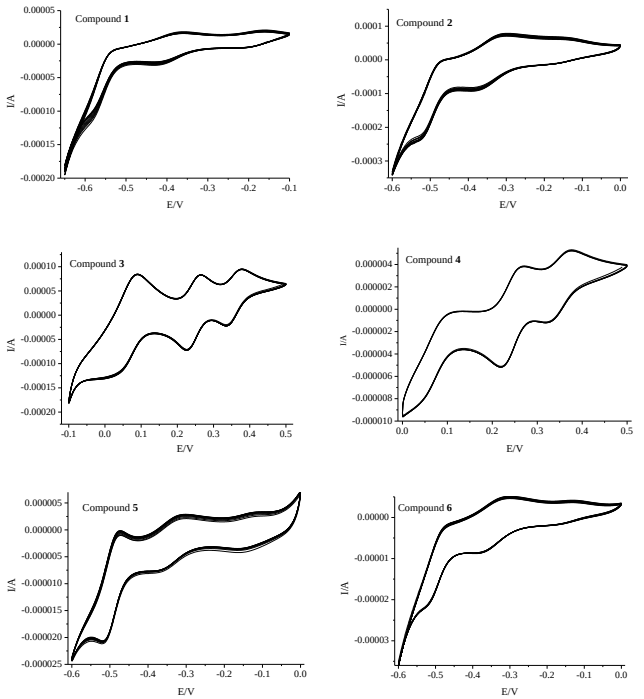

Fig. 9 cyclic voltammograms of DMSO solutions of compound **1-4**.

The cyclic voltammogram of **1**-CPE in 1mol/L H_2SO_4 solution at the scan rate of 100mV·s^{-1} was shown in Fig. 9. It is clearly seen that in the potential range -650 to -100mV, three pairs of redox peaks appeared. Mean peak potentials $E_{1/2}=(E_{pa}+E_{pc})/2$ were -555, -390 and -182mV. The cyclic voltammograms of **2**-CPE, **5**-CPE and **6**-CPE in 1mol/L H_2SO_4 solution at the scan rate of 100mV·s^{-1} are presented in the potential range of -600 to 0mV (Fig. 9), which exhibits similar redox peaks with half-wave potentials ($E_{1/2}=(E_{pa}+E_{pc})/2$) at -501, -344, -147mV, -496, -334, -134mV, and -496, -343, -143mV, respectively. The redox peaks correspond to one two-electron and two consecutive one-electron processes of W in compounds **1**, **2**, **5** and **6**, respectively.[19]

The cyclic voltammograms of **3**-CPE and **4**-CPE in 1mol/L H_2SO_4 solutions at the scan rate of 100mV·s-1 are presented in the potential range of -100 to 500mV (Fig. 9). There exist three

reversible redox peaks with half-wave potentials at 60, 245 and 357mV for **3**-CPE, half-wave potentials at 70, 246 and 350mV **4**-CPE, respectively. The redox peaks correspond to three two-electron processes of Mo in compounds **3** and **4**.[15]

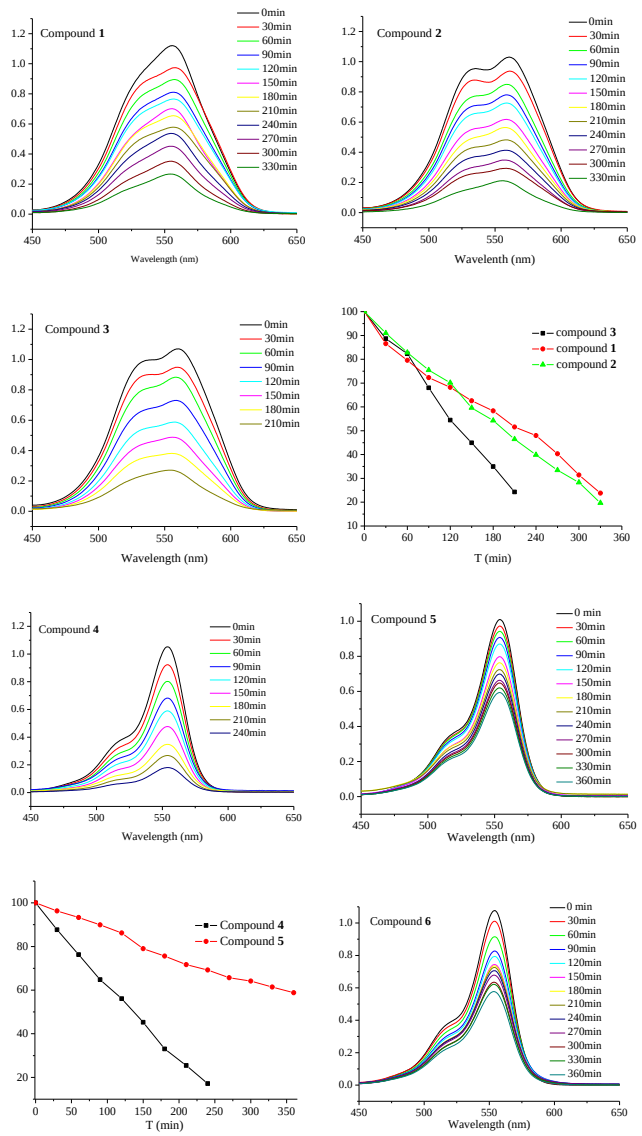

Fig. 10 photodegradation properties of compounds **1**-**6**.

RhB is a typical dye contaminant that can be used for evaluating the activity of photocatalysts for the purification of waste water.[20] The performance of compounds **1-4** for photocatalytic degradation of RhB has been investigated. In a typical process, 1.4×10^{-3}mmol compound **1** (5mg), **2** (5mg), **3** (3.5mg) or **4** (3.6mg) was grounded for about 10min with an agate mortar to obtain a fine powder, and then the powder was dispersed in 100 mL rhodamine B (RhB) solutions (3.0×10^{-5}mol·L^{-1} for compounds **1-3** and 1.0×10^{-5}mol·L^{-1} for compound **4**). The suspension was agitated in an ultrasonic bath for 20min in the dark and then magnetically stirred in the dark for about 30min. The suspension was finally exposed to irradiation from a 400W Xe lamp at a distance of about 4-5 cm between the liquid surface and the lamp. The suspension was stirred during irradiation at a stirring rate of about 790-800 rpm. At 30min intervals, 5mL of samples were taken out from the beaker, which was clarified by centrifugation at 10000 rpm for 5 min, and subsequently analyzed by UV-visible spectroscopy (Fig. 10). The photodegradation process of RhB without any photocatalyst has been studied for comparison, and only 23% of RhB was photodegraded after 360min. Changes in C_t/C_0 plot of RhB solutions versus reaction time were shown in Fig. 10. Compared with RhB without any photocatalyst, the absorption peaks of compounds **1-6** decreased upon irradiation, indicating that these compounds have photocatalysis properties. It also reveals that compounds **1-6** are photocatalysts for photocatalytic degradation of RhB.

Fig. 10 shows the reaction results of photodegradations of RhB over various catalysts at room temperature. As expected, all the catalysts are active for the photodegradation of RhB. Compound **1** catalyst shows the activity with 53.5% conversion after 210min. Compound **2** shows a lower activity with 48.5% conversion. Nevertheless, compound **3** shows a higher conversion of 75.7% after 210min. with increasing reaction time and the conversions of RhB reaches up to about 80% for compounds **1** and **2** after 330min. Compound **4** shows a high conversion (82.9%) after 240min. Compounds **5** and **6** shows lower conversions (58.8% for compound **5** and 53.5% for compound **6**) even after 360min.

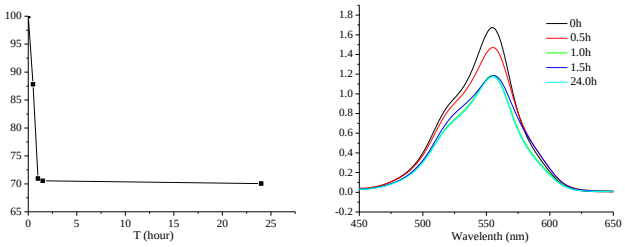

Fig. 11 absorption property for RhB of compound **1**.

Compounds **1-3** also exhibit strong rapid absorption properties for RhB. As shown in Fig. 11, the RhB absorption property of compound **1** was described detailedly as an example. About 30% RhB was absorbed after 1h in the dark, and then no more RhB was absorbed even after about 24h. However, compound **4** did not exhibit RhB absorption property at all; almost no RhB was absorbed after 0.5h in the dark.

Compounds **1**, **2** and **3** are isomorphous and isostructural, they contain identical transition metal ions, organic moieties and identical packing structures, the only difference between them is the Keggin species, it is $[H_2SiW_{12}O_{40}]^{2-}$ in compound **1,** $[H_2GeW_{12}O_{40}]^{2-}$ in compound **2** and $[H_2SiMo_{12}O_{40}]^{2-}$ in compound **3**. The photocatalytic reaction occurs in the adsorbed phase (on the surface of the catalyst), and the model of activation of the catalyst is photonic activation by exciting the POM with light energy higher than the band gap of the POM, which leads to an intramolecular charge transfer and the formation of the excited-state species (POM)*.[21] We have carefully discussed that the first reason for different RhB conversions using different POM-based catalysts should be the different POMs in them.[22] The second main reason should be perhaps ascribed to the different packing structures of POM-based catalysts.[22] Therefore, it is very hard for chemists to determine which one POM species has a higher degradation property, for the POMs in some catalysts are same, but the packing structures of the catalysts perhaps are not, thus, it is hard to distinguish it is the POM or the packing structure who plays the main role in the degradation process.

Fortunately, compounds **1**, **2** and **3** are isomorphous and isostructural, the packing structures of the three are same to one another. Therefore, the different RhB conversions using compounds **1**, **2** or **3** as catalysts should be only due to the

different POMs they contained. The comparison of RhB conversions using compounds **1, 2** or **3** as catalysts is described as below: compound **1**≈compound **2**<compound **3**. Thus, we can concluded that the POM degradation ability for RhB is: $[H_2SiW_{12}O_{40}]^{2-}$≈$[H_2GeW_{12}O_{40}]^{2-}$<$[H_2SiMo_{12}O_{40}]^{2-}$. For the only difference between compounds **1** and **3** are the metal ions, we can concluded that the molybdate POM has stronger degradation ability for RhB than the tungstate one. For the only difference between compounds **1** and **2** is the central heteroatoms, we can conclude that the POM central heteroatom has not fatal influence to its degradation ability.

Compounds **4** and **5** are isomorphous and isostructural with each other, too, RhB conversions using compounds **4** or **5** as catalysts are: compound **4** > compound **5**. Compound **4** is based on $[SiMo_{12}O_{40}]^{4-}$, and compound **5** is based on $[GeW_{12}O_{40}]^{4-}$. The relationship between compounds **4** and **5** is just similar to that between compounds **3** and **1**. Therefore, the catalytic results using compounds **4** and **5** as catalysts further demonstrated that the molybdate POM has stronger degradation ability for RhB than the tungstate one.

As mentioned above, it is hard to compare the degradation abilities of compounds **1-3** with those of compounds **4-5** or compound **6**. Wang[23] and Wang[15, 24] have also reported that the conversions of RhB over different compounds even containing identical Keggin species may not be same.

Conclusions

Six new organic-inorganic hybrid compounds based on the keggin-type polyoxoanion, namely $[Cu(pic)_2][H_2XM_{12}O_{40}]\cdot 2Hapy\cdot 2apy$ (X=Si, M=W for **1**, X =Ge, M =W for **2** and X=Si, M=Mo for **3**), Cu(2,2'-bpy)$_2$][Cu(2,2'-bpy)(H_2O)][Cu(pic)$_2]_{0.5}[XM_{12}O_{40}]\cdot nH_2O$ (X=Si, M=Mo, n=0.5 for **4**, X=Ge, M=W, n=1 for **5**), $[Cu(phen)(H_2O)]_2[Cu(pic)_2][GeW_{12}O_{40}]\cdot 2.5H_2O$ (**6**) have been synthesized and characterized. Compounds **1-3** are excellent photocatalysts for photocatalytic degradation of RhB and also exhibit strong absorption properties for RhB. Compound **4** is also an excellent photocatalyst for photocatalytic degradation of RhB but does not exhibit the absorption property for RhB. Compounds **5** and **6** also exhibit photocatalytic activity for photocatalytic degradation of RhB.

Acknowledgements

This work was supported by National Natural Science Foundation of China under Grant No. 21003056

Notes and references

[a] *College of Chemistry and State Key Laboratory of Inorganic Synthesis and Preparative Chemistry, Jilin University, Changchun, Jilin, 130023. E-mail:cuixb@mail.jlu.edu.cn.*

[b] Address here.

[c] Address here.

† Footnotes should appear here. These might include comments relevant to but not central to the matter under discussion, limited experimental and spectral data, and crystallographic data.

Electronic Supplementary Information (ESI) available: [details of any supplementary information available should be included here]. See DOI: 10.1039/b000000x/

1. a) M. T. Pope and A. Müller, *Polyoxometalates: From Platonic Solids to Anti-Retro Viral Activity*, Kluwer, Dordrecht, The Netherlands, 1994; b) M. T. Pope and A. Müller, *Angew. Chem., Int. Edit. Engl.*, 1991, **30**, 34; c) M. T. Pope, *Heteropoly and Isopoly Oxometalates*, Springer, Berlin, 1983; d) T. Yamase and M. T. Pope, *Polyoxometalate Chemistry for Nano-Composite Design*, the Netherlands, Kluwer, Dordrecht, 2002; e) C. L. Hill, *Chem. Rev.*, 1998, **98**, 1; f) D. L. Long, R. Tsunashima and L. Cronin, *Angew. Chem. Int. Ed. Engl.*, 2010, **49**, 1736; g) D. L. Long, E. Burkholder and L. Cronin, *Chem. Soc. Rev.*, 2007, 105; h) A. Proust, R. Thouvenot and P. Gouzerh, *Chem. Commun.*, 2008, 1837; i) A. Dolbecq, E. Dumas, C. R. Mayer and P. Mialane, *Chem. Rev.*, 2010, **110**, 6009.
2. a) J. Berzelius, *Poggendorff's, Ann. Phys.*, 1826, **6**, 369; b) J. F. Keggin, *Nature*, 1993, **131**, 908.
3. I. M. Mbomekalle, R. Cao, K. I. Hardcastle, C. L. Hil, M. Ammam, B. Keita, L. Nadjo and T. M. Anderson, *C. R. Chimie*, 2005, **8**, 1077.
4. a) A. Proust, B. Matt, R. Villanneau, G. Guillemot and G. L. P. Guozerh, *Chem. Soc. Rev.*, 2012, **41**, 7605; b) J. Zhang, F. P. Xiao, J. Hao and Y. G. Wei, *Dalton Trans.*, 2012, **41**, 3599; c) P. J. Hagrman, D. Hagrman and J. Zubieta, *Angew. Chem. Int. Edit*, 1999, **38**, 2638.
5. a) X. B. Cui, J. Q. Xu, H. Meng, S. T. Zheng and G. Y. Yang, *Inorg. Chem.*, 2004, **43**, 8005; b) H. Y. Guo, Z. F. Li, D. C. Zhao, Y. Y. Hu, L. N. Xiao, X. B. Cui, J. Q. Guan and J. Q. Xu, *Crystengcomm.*, 2014, **16**, 2251; c) S. Y. Shi, Y. Chen, J. N. Xu, Y. C. Zou, X. B. Cui, Y. Wang, T. G. Wang, J. Q. Xu and Z. M. Gao, *Crystengcomm.*, 2010, **12**, 1949; d) L. M. Wang, Y. Wang, Y. Fan, L. N. Xiao, Y. Y. Hu, Z. M. Gao, D. F. Zheng, X. B. Cui and J. Q. Xu, *crystengcomm.*, 2014, **16**, 430; e) L. N. Xiao, Y. Y. Hu, L. M. Wang, Y. Wang, J. N. Xu, H. Ding, X. B. Cui and J. Q. Xu, *Crystengcomm.*, 2012, **14**, 8589-8598; f) L. N. Xiao, Y. Y. Hu, L. M. Wang, Y. Wang, J. N. Xu, H. Ding, X. B. Cui and J. Q. Xu, *Crystengcomm.*, 2012, **14**, 8589; g) L. N. Xiao, J. N. Xu, Y. Y. Hu, L. M. Wang, Y. Wang, H. Ding, X. B. Cui and J. Q. Xu, *Dalton Trans.*, 2013, **42**, 5247; h) C. L. Pan, J. Q. Xu, G. H. Li, X. B. Cui, L. Ye and G. D. Yang, *Dalton Trans.*, 2003, 517; i) S. Y. Shi, Y. H. Sun, Y. Chen, J. N. Xu, X. B. Cui, Y. Wang, G. W. Wang, G. D. Yang and J. Q. Xu, *Dalton Trans.*, 2010, **39**, 1389; j) S. Y. Shi, Y. Wang, X. B. Cui, G. W. Wang, G. D. Yang and J. Q. Xu, *Dalton Trans.*, 2009, **31**, 6099.
6. a) L. Yuan, C. Qin, X. L. Wang, E. B. Wang and S. Chang, *Eur. J. Inorg. Chem.*, 2008, 4936; b) J. Tao, X. M. Zhang, M. L. Tong and X. M. Chen, *J. Chem. Soc., Dalton Trans.*, 2001, 770; c) L. Lisnard, A. Dolbecq, P. Mialane, J. Marrot, E. Codjovi and F. Sécheresse, *Dalton Trans.*, 2005, 3913; d) H. Jin, Y. F. Qi, E. B. Wang, Y. G. Li, C. Qin, X. L. Wang and S. Chang, *Eur. J. Inorg. Chem.*, 2006, 4541; e) H. Jin, Y. F. Qi, E. B. Wang, Y. G. Li, X. L. Wang, C. Qin and S. Chang, *Cryst. Growth Des.*, 2006, **6**, 2693.
7. a) S. Reinoso, P. Vitoria, L. Felices, L. Lezama and J. M. Gutiérrez-Zorrilla, *Inorg. Chem.*, 2006, **45**, 108; b) S. Reinoso, P. Vitoria, J. M. Gutiérrez-Zorrilla, L. Lezama, L. S. Felics and J. I. Beitia, *Inorg. Chem.*, 2005, **44**, 9731; c) S. Reinoso, P. Vitoria, L. Lezama, A. Luque and J. M. Gutiérrez-Zorrilla, *Inorg. Chem.*, 2003, **42**, 3709; d) X. Y. Zhao, D. D. Liang, S. X. Liu, C. Y. Sun, R. G. Cao, C. Y. Gao, Y. H. Ren and Z. M. Su, *Inorg. Chem.*, 2008, **47**, 7133; e) Y. Yang, S. X. Liu, C. C. Li, S. J. Li, G. J. Ren, F. Wei and Q. Tang, *Inorg. Chem. Commun.*, 2012, **17**, 54; f) Q. X. Han, P. T. Ma, J. W. Zhao, J. P. Wang and J. Y. Niu, *Inorg. Chem. Commun.*, 2011, **14**, 767.
8. a) C. Z. Lu, C. D. Wu, H. H. Zhuang and J. S. Huang, *Chem. Mater.*, 2002, **14**, 2649; b) S. W. Zhang, Y. X. Li, Y. Liu, R. G. Cao, C. Y. Sun, H. M. Ji and S. X. Liu, *J. Mol. Struct.*, 2009, **920**, 284; c) X. L. Wang, Q. Gao, G. C. Liu, H. Y. Lin, A. X. Tian and J. Li, *Inorg. Chem. Commun.*, 2011, **14**, 745; d) Z. K. Qu, K. Yu, Z. F. Zhao, Z. H. Su, J. Q. Sha, C. M. Wang and B. B. Zhou, *Dalton Trans.*, 2014, **43**, 6744.
9. a) A. Dolbecq, P. Mialane, L. Lisnard, J. Marrot and F. Sécheresse, *Chem. Eur. J.*, 2003, **9**, 2914; b) P. Mialane, A. Dolbecq and F. Sécheresse, *Chem. Commun.*, 2006, 3477; c) B. Nohra, H. E. Moll, L. M. R. Albelo, P. Mialane, J. Marrot, C.

Mellot-Draznieks, M. O'Keeffe, R. N. Biboum, J. Lemaire, B. Keita, L. Nadjo and A. Dolbecq, *J. Am. Chem. Soc.*, 2011, **133**, 13363; d) G. Rousseau, O. Oms, A. Dolbecq, J. R. M. Marrot and P. Mialane, *Inorg. Chem.*, 2011, **50**, 7376; e) S. T. Zheng, J. Zhang and G. Y. Yang, *Angew. Chem. Int. Ed. Engl.*, 2008, **47**, 3909.

10. D. C. Zhao, Y. Y. Hu, H. Ding, H. Y. Guo, X. B. Cui, X. Zhang, Q. S. Huo and J. Q. Xu, *Dalton Trans.*, 2015, **44**, 8971.
11. G. Sheldrick, *Acta Crystallogr., Sec. A.*, 2008, **64**, 112.
12. L. Farrugia, *J. Appl. Crystallogr.*, 2012, **45**, 849.
13. I. D. Brown, Academic Press, New York, 1981.
14. a) X. B. Cui, Y. Q. Sun and G. Y. Yang, *Inorg. Chem. Commun.*, 2003, **6**, 259; b) X. B. Cui, J. Q. Xu, Y. Li, Y. H. Sun and G. Y. Yang, *Eur. J. Inorg. Chem.*, 2004, 1051.
15. X. L. Wang, N. Han, H. Y. Lin, A. X. Tian, G. C. Liu and J. W. Zhang, *Dalton Trans.*, 2014, **43**, 2052.
16. H. Y. An, Y. G. Li, E. B. Wang, D. R. Xiao, C. Y. Sun and L. Xu, *Inorg. Chem.*, 2005, **44**, 6062.
17. a) P. C. Yin, T. Li, R. S. Forgan, C. Lydon, X. B. Zuo, Z. X. N. Zheng, B. Lee, D. L. Long, L. Cronin and T. B. Liu, *J. Am. Chem. Soc.*, 2013, **135**, 13425; b) C. P. Pradeep, F. Y. Li, C. Lydon, H. N. Miras, D. L. Long and L. Cronin, *chem. Eur. J.*, 2011, **17**, 7472.
18. C. Rocchiccioli-Deltcheff, M. Fournier, R. Franck and R. Thouvenot, *Inorg. Chem.*, 1983, **22**, 207-216.
19. a) S. Q. Liu, Z. Shi and S. J. Dong, *Electroanalysis*, 1998, **10**, 891; b) M. G. Liu, P. P. Zhang, J. Peng, H. X. Meng, X. Wang, M. Zhu, D. D. Wang, C. L. Meng and K. Alimaje, *Cryst. Growth Des.*, 2012, **12**, 1273; c) A. X. Tian, J. Ying, J. Peng, J. Q. Sha, Z. M. Su, H. J. Pang, P. P. Zhang, Y. Chen, M. Zhu and Y. Shen, *Cryst. Growth Des.*, 2010, **10**, 1104.
20. a) J. Lü, J. X. Lin, X. L. Zhao and R. Cao, *Chem. Commun.*, 2012, **48**, 669; b) J. Q. Sha, J. W. Sun, M. T. Li, C. Wang, G. M. Li, P. F. Yan and L. J. Sun, *Dalton Trans.*, 2013, **42**, 1667.
21. a) H. Fu, Y. G. Li, Y. Lu, W. L. Chen, Q. Wu, J. X. Meng, X. L. Wang, Z. M. Zhang and E. B. Wang, *Cryst. Growth Des.*, 2011, **11**, 458; b) D. Y. Chen, A. Sahasrabudhe, P. Wang, A. Dasgupta, R. X. Yuan and S. Roy, *Dalton Trans.*, 2013, **42**, 10587.
22. L. N. Xiao, L. M. Wang, X. N. Shan, H. Y. Guo, L. W. Fu, Y. Y. Hu, X. B. Cui, K. C. Li and J. Q. Xu, *Crystengcomm.*, 2015, **17**, 1336.
23. Q. Lan, J. Zhang, Z. M. Zhang, Y. Lu and E. B. Wang, *Dalton Trans.*, 2013, **42**, 16602.
24. X. L. Wang, D. Zhao, A. X. Tian and J. Ying, *Dalton Trans.*, 2014, **43**, 5211.